High-Spatial-Resolution Time-Domain Simultaneous Strain and Temperature Sensor Using Brillouin Scattering and Birefringence in a Polarization-Maintaining Fiber

Yongkang Dong, Liang Chen, and Xiaoyi Bao, *Senior Member, IEEE*

***Abstract*—We report on a high-spatial-resolution simultaneous strain and temperature measurement in time domain through measuring Brillouin frequency shift (BFS) and birefringence-induced frequency shift (BireFS) in a polarization-maintaining fiber. High-spatial-resolution BFS and BireFS measurement are obtained through differential pulsewidth pair Brillouin optical time-domain analysis and a local Brillouin grating, respectively. Simultaneous strain and temperature measurement with a spatial resolution of 20 cm is demonstrated in a 6-m Panda fiber. The temperature and strain accuracy is 0.4 °C and 9 $\mu\varepsilon$, and their range can be up to 700 °C and 14 mε, respectively.**

***Index Terms*—Birefringence, Brillouin scattering, polarization-maintaining fiber (PMF), strain measurement, temperature measurement.**

I. Introduction

THE Brillouin-scattering-based distributed fiber sensor has been developed for two decades and shows capability of measuring strain and temperature for structure health monitoring. However, since both strain and temperature can produce a Brillouin frequency shift (BFS) change, the Brillouin-based sensor suffers from the cross sensitivity. Normally, it cannot be determined that a BFS change is induced by a change in temperature or strain. A practical discrimination method is to introduce an additional measurable parameter, which has an independent relationship with strain and temperature. Brillouin power was introduced in a Brillouin optical time-domain reflectometer; meanwhile, it reduced the measurement precision considerably [1]. In [2], birefringence in a polarization-maintaining fiber (PMF) was introduced as the second parameter to discriminate the strain and temperature. Compared with the positive strain and temperature coefficients of BFS, the birefringence has a positive strain coefficient and negative temperature coefficient, which ensures a high discrimination precision [2]. More recently, the same authors realized the discrimination of strain and temperature with a high-spatial-resolution of 10 cm in correlation domain [3].

In this letter, we realized simultaneous strain and temperature measurement with a high spatial resolution in time domain using Brillouin scattering and birefringence in a PMF. For BFS measurement, we used the differential pulsewidth pair Brillouin optical time-domain analysis (DPP-BOTDA) to realize a high spatial resolution [4], [5]; here a high spatial resolution of 20 cm is achieved by using a pulsewidth difference of 2 ns and a narrowband Brillouin gain spectrum is obtained from a pulse pair of 30/28 ns. For birefringence-induced frequency shift (BireFS) measurement, two short pump pulses (2 ns) are used to generate a local Brillouin grating and thus get a high spatial resolution of 20 cm [6], [7]. A simultaneous strain and temperature measurement was demonstrated over 6-m Panda fiber with a spatial resolution of 20 cm. The temperature and strain accuracy is 0.4 °C and 9 $\mu\varepsilon$, and their range can be up to 700 °C and 14 mε.

II. Sensing Principles

Brillouin scattering is an inelastic light scattering with acoustic phonons and undergoes a frequency shift after collision. BFS is given by [8]

$$\nu_B = 2nV_a/\lambda \tag{1}$$

where n is the refractive index, V_a is the velocity of acoustic wave, and λ is the light wavelength in vacuum. It was found that the BFS increases with strain and temperature, which provides a mechanism to realize a distributed sensing.

In a PMF, a Brillouin grating can be excited in one axis of PMF through two counterpropagating pump lights (pump1 and pump2) with a frequency offset of BFS. This Brillouin grating spectrum can be mapped by launching a probe pulse following pump2 pulse into the other axis. A maximum reflected probe signal could be obtained when frequency offset between pump2 and the probe satisfies the phase-matching condition, and can be given by [7]

$$\nu_{\mathrm{Bire}} = \Delta n\nu/n_g \tag{2}$$

where Δn is the phase modal birefringence, n_g is the group refractive index, and ν is the light frequency. Temperature and strain both can alter the birefringence of the PMF, and it was found that the BireFS increases with the strain and decreases with temperature, which provides another uncorrelated mechanism to measure the temperature and strain change.

Manuscript received March 15, 2010; revised June 15, 2010; accepted June 25, 2010. Date of publication July 08, 2010; date of current version September 01, 2010. This work was supported by the Natural Science and Engineering Research council of Canada through a discovery and strategic grant and by the Canada Research Chair Program.

The authors are with the Department of Physics, University of Ottawa, Ottawa, ON, K1N 6N5, Canada (e-mail: aldendong@gmail.com; Liang.Chen@uottawa.ca; xbao@uottawa.ca).

Color versions of one or more of the figures in this letter are available online at http://ieeexplore.ieee.org.

Digital Object Identifier 10.1109/LPT.2010.2056678

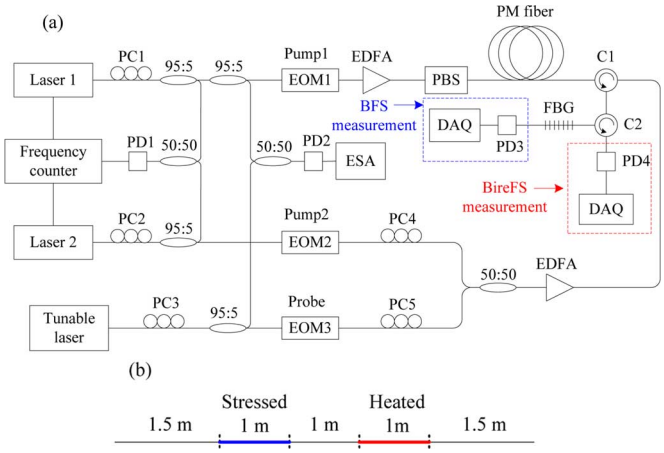

Fig. 1. (a) Experimental setup. PC: polarization controller; EOM: electrooptic modulator; PBS: polarization beam splitter; C: circulator; PD: photodetector; EDFA: erbium-doped fiber amplifier; ESA: electrical spectrum analyzer; FBG: fiber Bragg grating; DAQ: data acquisition. (b) Layout of the 6-m sensing fiber.

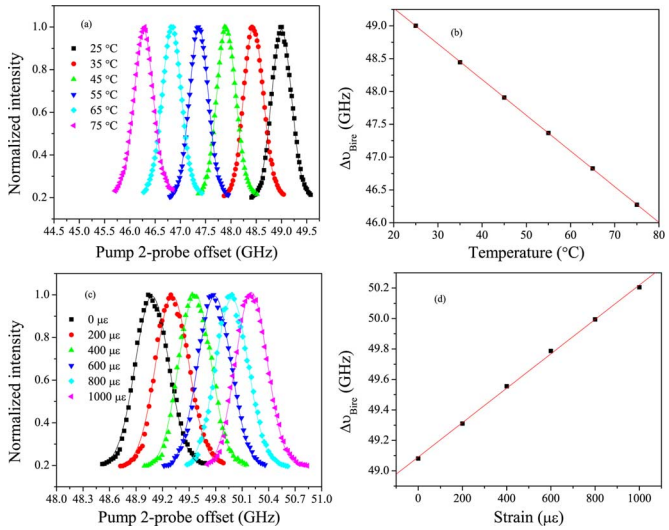

Fig. 2. (a) Measured Brillouin grating spectra at different temperatures and (b) the dependence of BireFS on temperature; (c) measured Brillouin grating spectra at different strains and (d) the dependence of BireFS on strain.

The strain and the temperature can then be uniquely determined by the measured BFS and BireFS, and can be given by [2]

$$\begin{bmatrix} \Delta\varepsilon \\ \Delta T \end{bmatrix} = \frac{1}{C_B^{\varepsilon} C_{\text{Bire}}^{T} - C_B^{T} C_{\text{Bire}}^{\varepsilon}} \times \begin{bmatrix} C_{\text{Bire}}^{T} & -C_B^{T} \\ -C_{\text{Bire}}^{\varepsilon} & C_B^{\varepsilon} \end{bmatrix} \begin{bmatrix} \Delta\nu_B \\ \Delta\nu_{\text{Bire}} \end{bmatrix} \quad (3)$$

where $\Delta\varepsilon$ and ΔT are changes in strain and temperature, respectively; $C_B^{\varepsilon}, C_B^{T}, C_{\text{Bire}}^{\varepsilon}$, and C_{Bire}^{T} are coefficients to strain and temperature related to BFS and BireFS, respectively. Here $C_B^{\varepsilon}, C_B^{T}$, and $C_{\text{Bire}}^{\varepsilon}$ have a positive sign, while C_{Bire}^{T} has a negative sign, so $C_B^{\varepsilon} C_{\text{Bire}}^{T} - C_B^{T} C_{\text{Bire}}^{\varepsilon}$ is a large value, which ensures a high discrimination accuracy [2].

III. Experimental Setup

The experimental setup is shown in Fig. 1. For BFS measurement, two narrow linewidth fiber lasers operating at 1550 nm are used, and their frequency difference is locked by a phase locking loop in a frequency counter. Laser 1 provides CW pump and laser 2 provides probe pulse.

For BireFS measurement, laser 1 and laser 2 provide pump1 and pump2, respectively. The frequency difference between pump1 and probe is monitored and recorded by a high-speed detector with a bandwidth of 45 GHz and a 44-GHz electrical spectrum analyzer. Three high extinction-ratio (ER) EOMs are used to generate a 2-ns pump1 pulse, a 2-ns pump2 pulse, and a 6-ns probe pulse with the ER higher than 45 dB. The powers of the pump1 pulse, pump2 pulse, and probe pulse in the PMF are about 200 mW, 30 W, and 30 W, respectively. Two pump pulses are launched into the slow axis and the delay between them is well controlled to create a local Brillouin grating at a specific location. The probe pulse is launched into the fast axis with a time delay of 2 ns with respect to the pump2 pulse, where the delay is chosen to separate the transmitted pump1 pulse and reflected signal in the time domain. A tunable fiber Bragg grating with a bandwidth of 0.2 nm is used to filter out the transmitted pump1 pulse. A 6-m Panda fiber is used as sensing fiber with a BFS of 10.871 GHz at room temperature.

IV. Measured Results and Discussion

First, we measured the dependences of BFS on temperature and strain, and the temperature and strain coefficients are $C_B^{T} = 1.12$ MHz/°C and $C_B^{\varepsilon} = 0.0482$ MHz/$\mu\varepsilon$, respectively, which agree with the results in previous works [9].

Then we measured the dependences of BireFS on temperature and strain, and the results are shown in Fig. 2. The Brillouin grating spectra were obtained using the 2-ns pump1, 2-ns pump2, and 6-ns probe. A Brillouin grating spectrum with a two-peak structure was observed previously [7]. In this letter, we found that it is induced by the leakage of the pump1 pulse, which causes a dip at the central of the spectrum showing a two-peak structure. Using three high ER (ER >45 dB) modulators, one-peak Gaussian Brillouin grating spectrum is obtained, as shown in Fig. 2(a) and (c). The measured spectrum agrees well with a Gaussian profile and its FWHM width is ~640 MHz. The fitting temperature and strain coefficients of BireFS are $C_{\text{Bire}}^{T} = -54.38$ MHz/°C and $C_{\text{Bire}}^{\varepsilon} = 1.13$ MHz/$\mu\varepsilon$, respectively.

Simultaneous measurement of strain and temperature is performed using a 6-m Panda fiber with 1-m stressed segment, 1-m heated segment, and 1-m segment at room temperature and loose state in between, which is shown in Fig. 1(b). The applied strain is about 670 $\mu\varepsilon$ and the heated temperature is higher than room temperature by 30 °C.

DPP-BOTDA is used to perform BFS measurement. A 30/28-ns pulse pair is used and the spatial resolution is 20 cm, which is determined by 2-ns pulsewidth difference. The BFS is obtained through one-peak Lorentz fitting and the BFS difference (subtracting the BFS at room temperature and loose state) is shown in Fig. 3(a). The fitting uncertainty of BFS is 0.4 MHz, corresponding to a δT of 0.36 °C and a $\delta\varepsilon$ of 8.3 $\mu\varepsilon$. For BireFS measurement, the spatial resolution is determined by the effective length of the Brillouin grating, which is about

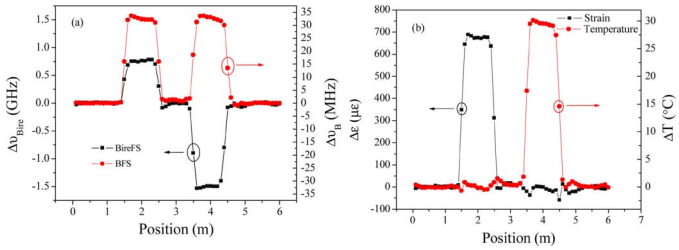

Fig. 3. (a) Measured $\Delta\nu_{\mathrm{Bire}}$ and $\Delta\nu_B$ and (b) calculated temperature and strain.

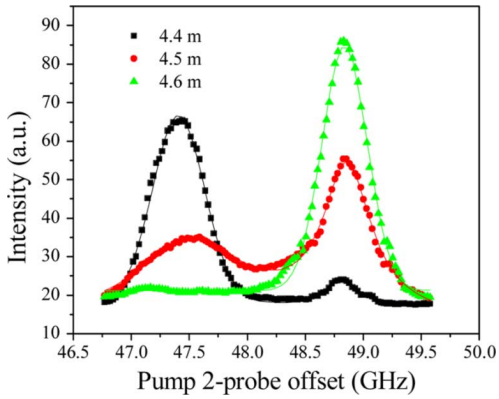

Fig. 4. Measured Brillouin grating spectra at a transition region.

20 cm for 2-ns pump pulses. A longer 6-ns probe pulse is used to provide narrower measured Brillouin grating spectrum, and thus give better frequency accuracy. The BireFS difference (subtracting the BireFS at room temperature and loose state) is also shown in Fig. 3(a). At the transition region, a two-peak spectrum is observed due to the limitation of spatial resolution, and Fig. 4 shows the Brillouin grating spectra at a transition region from heated segment to nonheated segment (4.4–4.6 m). With a two-peak spectrum, the BireFS is calculated through the power weight of intensity of individual peak. The fitting uncertainty of BireFS is 3 MHz, corresponding to a δT of 0.06 °C and a $\delta\varepsilon$ of 2.7 $\mu\varepsilon$. Note that the BireFS provides higher precision with respect to BFS, so that the discrimination accuracy is limited by the uncertainty of BFS.

Using measured strain, temperature coefficients, and BFS and BireFS differences, we can simultaneously get the distributed temperature and strain along the sensing fiber, which are shown in Fig. 3(b). It is clear that the temperature and strain are discriminated from each other except at the transition regions, where the uncertainty in BFS and BireFS measurement due to the spatial resolution brings error.

The measurement range of this scheme is limited by the BireFS measurement, where the intensity of the Brillouin grating can decrease with increasing detuning induced by large temperature or strain change. We investigated the intensity of Brillouin grating at different offset between pump1 and pump2, from 10.5 to 11.2 GHz, and the results are shown in Fig. 5. Due to the broadband spectrum of 2-ns pump pulses, the intensities are all larger than the 60% of the peak value within 700 MHz, which allows a temperature measurement range of 700 °C and

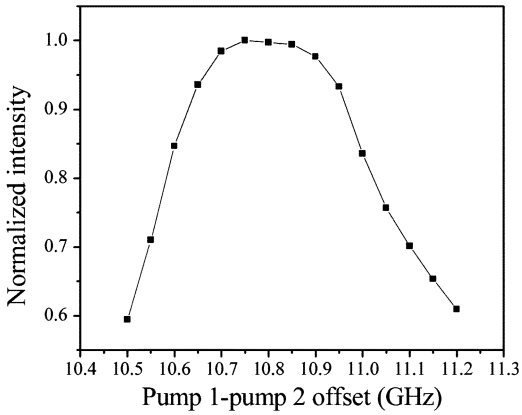

Fig. 5. Intensity of Brillouin grating spectrum versus the pump1–pump2 offset.

a strain measurement range of 14 mε with a fix frequency offset between two pump waves.

In summary, we have demonstrated a time-domain high-spatial-resolution discrimination of strain and temperature using Brillouin scattering and birefringence in a PMF. High ER modulators are used to remove the impact of dc leakage and thus obtain a one-peak Brillouin grating spectrum. Simultaneous strain and temperature measurement with a spatial resolution of 20 cm is demonstrated in a 6-m Panda fiber with a measurement accuracy of 0.4 °C and 9 $\mu\varepsilon$ and a measurement range of up to 700 °C and 14 mε, respectively.

ACKNOWLEDGMENT

Y. Dong would like to thank Dr. H. Liang for help on the experiment.

REFERENCES

[1] T. R. Parker, M. Farhadiroushan, V. A. Handerek, and A. J. Rogers, "A fully distributed simultaneous strain and temperature sensor using spontaneous Brillouin backscatter," *IEEE Photon. Technol. Lett.*, vol. 9, no. 7, pp. 979–981, Jul. 1997.

[2] W. Zou, Z. He, and K. Hotate, "Complete discrimination of strain and temperature using Brillouin frequency shift and birefringence in a polarization-maintaining fiber," *Opt. Express*, vol. 17, pp. 1248–1255, 2009.

[3] W. Zou, Z. He, and K. Hotate, "Demonstration of Brillouin distributed discrimination of strain and temperature using a polarization-maintaining optical fiber," *IEEE Photon. Technol. Lett.*, vol. 22, no. 8, pp. 526–528, Apr. 15, 2010.

[4] W. Li, X. Bao, Y. Li, and L. Chen, "Differential pulse-width pair BOTDA for high spatial resolution sensing," *Opt. Express*, vol. 16, pp. 21616–21625, 2008.

[5] Y. Dong, X. Bao, and W. Li, "Differential Brillouin gain for improving the temperature accuracy and spatial resolution in a long-distance distributed fiber sensor," *Appl. Opt.*, vol. 48, pp. 4297–4301, 2009.

[6] Y. Dong, X. Bao, and L. Chen, "Distributed temperature sensing based on birefringence effect on transient Brillouin grating in a polarization-maintaining photonic crystal fiber," *Opt. Lett.*, vol. 34, pp. 2590–2592, 2009.

[7] Y. Dong, L. Chen, and X. Bao, "Truly distributed birefringence measurement of polarization-maintaining fibers based on transient Brillouin grating," *Opt. Lett.*, vol. 35, pp. 193–195, 2010.

[8] T. Horiguchi, K. Shimizu, T. Kurashima, M. Tateda, and Y. Koyamda, "Development of a distributed sensing technique using Brillouin scattering," *J. Lightw. Technol.*, vol. 13, no. 7, pp. 1296–1302, Jul. 1995.

[9] T. R. Parker, M. Farhadiroushan, V. A. Handerek, and A. J. Rogers, "Temperature and strain dependence of the power level and frequency of spontaneous Brillouin scattering in optical fibers," *Opt. Lett.*, vol. 22, pp. 787–789, 1997.